A ROBUST METHOD OF EXTRACTING ANGLE-DOMAIN COMMON-IMAGE GATHERS FROM SHOT-PROFILE WAVE EQUATION MIGRATION

JIANGJIE ZHANG

Institute of Geology and Geophysics, Chinese Academy of Sciences, Beijing 100029, China.

(Received January 6, 2012; revised version accepted May 22, 2012)

ABSTRACT

Zhang, J., 2012. A robust method of extracting angle-domain common-image gathers from shot-profile wave equation migration. *Journal of Seismic Exploration*, 21: 267-280.

Shot-profile pre-stack depth migration is quite attractive for sparse-shot wide-azimuth geometries. Meanwhile, angle-domain common-image gathers (ADCIGs) have become an essential tool in seismic processing. After revisiting the popular schemes of extracting ADCIGs, we present a robust method to estimate the incident-angle field and extract ADCIGs from shot-profile wave equation migration. The cosines of the incident-angle can be estimated from the ratios between the square roots of the angle-weighted image gathers' Laplacian operators and the amplitude values from the conventional common-image gathers. The angle-weighted image gathers can be extracted by multiplying an extra imaging weight including local propagation velocity and angular frequency in conventional shot-profile wave-equation migration process, while the conventional common-image gathers are obtained using the cross-correlation imaging condition. A stable division at selected wave crests with large amplitude ensures the stability and avoids noise interference. Finally, we separate the shot-domain common-image gathers (SDCIGs) into different angle bins using incident-angle field to extract ADCIGs. Numerical examples demonstrate that the method is stable and memory-efficient and independent of structural dips.

KEY WORDS: shot-profile wave equation migration, common-image gathers, incident-angle, structural dip.

0963-0651/12/$5.00

INTRODUCTION

Angle-domain common-image gathers (ADCIGs) are an effective tool for performing velocity analysis and have also been incorporated into studies of amplitude variation with angle (AVA) (Biondi, 2006). There are several methods to extract ADCIGs from wave equation migration (Sava and Fomel, 2005a,b; Shragge, 2012) and reverse time migration (Yoon et al., 2011; Zhang and McMechan, 2011). Since it can handle strong velocity heterogeneities and is computational efficiency compared to reverse time migration, the one-way wave equation migration is one of the most widely applied imaging methods in structurally complex areas.

Pre-stack wave equation migration can be applied either in shot-geophone migration or shot-profile migration. The former is based on the concept of survey-sinking and the wavefield is extrapolated with the double square-root equation (Claerbout, 1985). Because the image is extracted with the shot and geophone sinking, it is easy to estimate incident-angles and to obtain ADCIGs. In contrast, during shot-profile migration, the up-going and down-going wavefields are extrapolated separately with the single square-root equation, which makes the calculation of ADCIGs more complicated (Bleistein et al., 2001). In addition, shot-geophone migrations have a larger computational cost than shot-profile migration for wide-azimuth geometries when the number of shots is small compared to the number of offsets (Rickett and Sava, 2002). Thus, we consider to develop a method to obtain ADCIGs from shot-profile wave equation migration.

There are many methods to extract ADCIGs using shot-profile wave equation migration. In one approach, ADCIGs are extracted at each imaging point by applying the imaging condition after local plane wave decomposition for the incident and reflected wave (de Bruin et al., 1990; Xie and Wu, 2002). The huge calculations and memories involved prevent this method for practical applications. In a second approach, the ray tracing theory based on high-frequency approximation imposes limitations on the subsurface model (Lecomte, 2008). To ensure valid rays, the velocity model must be smoothed and vary slowly. Furthermore, the incident-angle information becomes structure-dependent: the gathers not only depend on the ray tracing but also on the structural dip. In a third approach, Sava and Fomel (2003, 2005) converted half-offset gathers to ADCIGs by a Radon-transform or slant-stack after imaging. The advantage of this approach is that it is independent of structural dip. However, it is limited by its huge memory cost, especially in the 3D case (Zhang et al., 2005, 2007). Another drawback of this approach is high-frequency loss, resulting from the Radon-transform or slant-stack, which reduces the image resolution.

In this paper, we present a new approach to estimate the incident-angle field from shot-domain common-image gathers (SDCIGs). We obtain conventional common-image gathers by shot-profile wave equation migration using the cross-correlation imaging condition. The angle-weight common-image gathers are obtained by multiplying an extra imaging weight including local propagation velocity and angular frequency in conventional imaging process. Then we apply a Laplacian operator to the angle-weight common-image gather and calculate their square roots. The cosines of the incident-angle can be estimated from the ratios between the square roots and the amplitude values from the conventional common-image gathers. Finally, we separate the SDCIGs into different angle bins using the incident-angle field to produce the ADCIGs. Comparing with Sava and Fomel's method, we generate only two images from a single-shot migration rather than generating outputs consisting of many cubes of half-offset gathers. In addition, we apply a stable division at selected wave crests with large amplitude to guarantee stability to ensure generality of the method.

METHODOLOGY

In this section, we first analyze the reflection geometry of a dipping reflector in a locally homogeneous medium (Fig. 1). A local reflector plane in {x,y,z} coordinates can be described as

$$x\cos\alpha + y\cos\beta + z\cos\gamma = d \quad , \tag{1}$$

where the angles α, β and γ of the direction cosines of the normal to the reflector satisfy

$$\cos^2\alpha + \cos^2\beta + \cos^2\gamma = 1 \quad . \tag{2}$$

For the reflection ray path geometry in Fig. 1, the reflection travel time measured on a horizontal surface above the reflector is (Slotnik, 1959; Levin, 1971)

$$t(h_x,h_y) = (2/v)\sqrt{[D^2 + h_x^2 + h_y^2 - (h_x\cos\alpha + h_y\cos\beta)^2]} \quad , \tag{3}$$

where D is the length of the line normal to reflector from the midpoint, shown as MN in Fig. 1

$$D = d - m_x\cos\alpha - m_y\cos\beta \quad , \tag{4}$$

m_x and m_y are the midpoint coordinates, h_x and h_y are the half-offset coordinates, and v is the propagation velocity. Note that the theoretical analysis

of angle gathers in downward continuation methods can be reduced to analyzing the geometry in the Fig. 1 in a locally homogeneous media. Thus the parameter v can be used as the local propagation velocity in the following derivation.

The incident/reflection angle θ is related to the previously introduced quantities by

$$\cos\theta = D/\sqrt{[D^2 + h_x^2 + h_y^2 - (h_x\cos\alpha + h_y\cos\beta)^2]} \quad , \tag{5}$$

Explicitly differentiating eq. (3) with respect to the midpoint and offset coordinates and utilizing eq. (5) leads to

$$\partial t/\partial m_x = -(2/v)\cos\theta\cos\alpha \quad , \tag{6}$$

$$\partial t/\partial m_y = -(2/v)\cos\theta\cos\beta \quad . \tag{7}$$

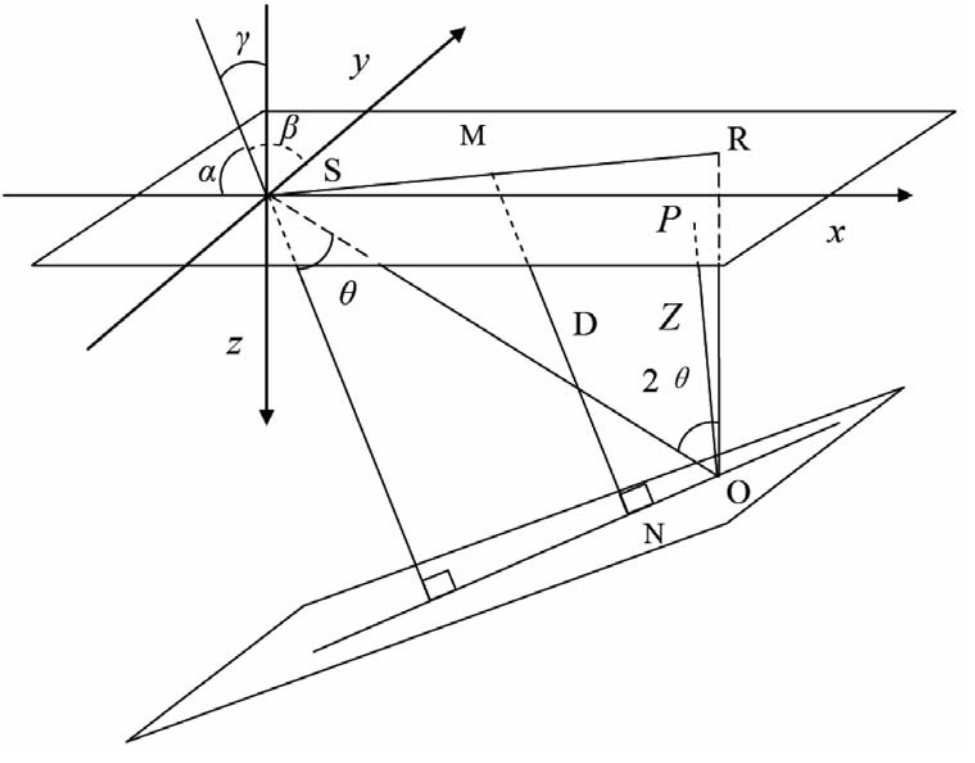

Fig. 1. Reflection geometry. S and R are the source and receiver positions at the surface. O is the reflection point. M is the midpoint form S to R. MN (D) is the length of the normal to the reflector from the midpoint.

Additionally, the travel time derivative with respect to the depth Z (OP) of the imaging point below observation surface is given by

$$\partial t/\partial Z = -(2/v)\cos\theta\cos\gamma \quad . \tag{8}$$

In the Fourier domain, each t_x derivative translates into $-k_x/\omega$ ratio, where k_x is the wavenumber in the x-direction and ω is the angular frequency. Then from eqs. (6), (7) and (8),

$$\cos\theta = (v/2\omega)\sqrt{(k^2_{m_x} + k^2_{m_y} + k^2_z)} \quad , \tag{9}$$

for incident-angle gathers. Since the Laplacian operator in the wavenumber domain is

$$\nabla^2 \overset{FFT}{\sim} k_x^2 + k_y^2 + k_z^2 \quad , \tag{10}$$

and the cross-correlation imaging condition is

$$I(\mathbf{x}) = \sum_{\mathbf{x}_s} \int P_U(\mathbf{x};\mathbf{x}_s;\omega)P_D^*(\mathbf{x};\mathbf{x}_s;\omega)d\omega \quad , \tag{11}$$

for the imaging location $\mathbf{x} = (x,y,z)$ and shot location $\mathbf{x}_s = (x_s,y_s,0)$, P_D is the down-going response to a source at $z = 0$, and P_U is the up-going wave that is the observed seismic data at the surface. We give a new imaging condition

$$I'(\mathbf{x}) = \sum_{\mathbf{x}_s} \int [v(\mathbf{x})/2\omega]P_U(\mathbf{x};\mathbf{x}_s;\omega)P_D^*(\mathbf{x};\mathbf{x}_s;\omega)d\omega \quad , \tag{12}$$

where $v(\mathbf{x})$ is the velocity at the imaging location. From eqs. (9), (10), (11) and (12), we obtain the cosine of the incident angle

$$\sqrt{[\nabla^2(I')]} \,/\, I = \{[v(\mathbf{x})/2\omega]\sqrt{(k^2_{m_x} + k^2_{m_y} + k^2_z)} \cdot I\} \,/\, I = \cos\theta \quad . \tag{13}$$

The method obtains the angle-weight common-image gathers by multiplying an imaging weight $v(\mathbf{x})/2\omega$ in conventional migration, which is efficient and memory-saving. The cosines of the incident-angle can be estimated from the ratios between the square roots of the angle-weighted image gathers' Laplacian operators and the amplitude values from the conventional common-image gathers. The drawback is that the relation (13) requires a division that may cause instability when the magnitude of I is small; hence we add a small quality ε to ensure stability

$$\cos\theta = \sqrt{[\nabla^2(I')]} \,/\, (I + \varepsilon) \quad . \tag{14}$$

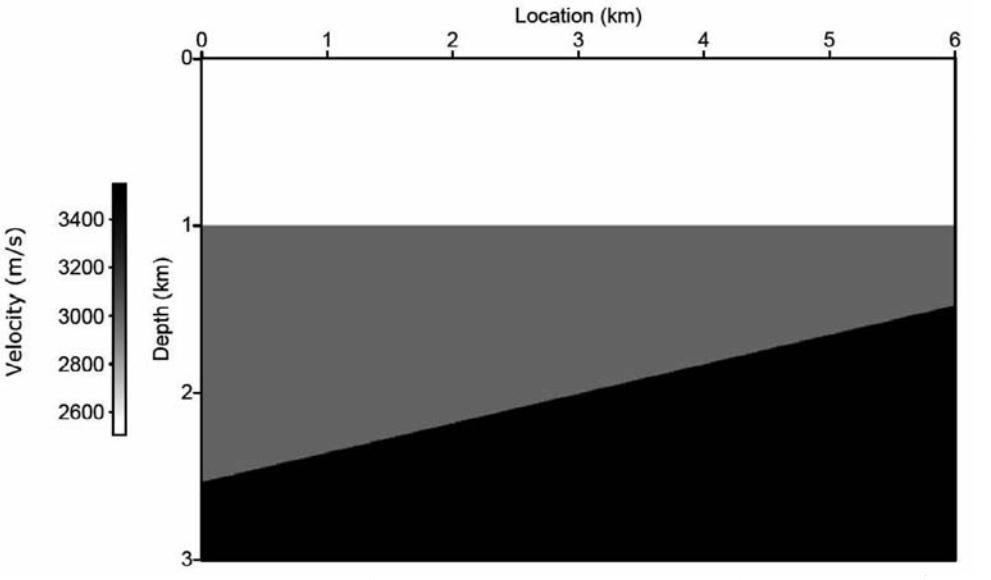

Fig. 2. Velocity model of simple reflective model.

Because of the Laplacian operator, when noise is present, eq. (14) will fail to compute an accurate incident/reflection angle. To overcome this, we can image the low-frequency part of the data to compute the incident-angle to avoid high-frequency noise artifacts. We also calculate the incident-angle by eq. (14) only at the wave crests above a threshold amplitude value such as the average amplitude in the gather, and other points are interpolated along vertical direction. To avoid computational errors, we abandon those irregular points when $\cos\theta > 1$. Finally, we smooth the cosines along the same depth level to ensure the continuity of the events in the gather, which will introduce acceptable errors in the incident-angle calculation, as shown in Fig. 3b. The algorithm can be summarized in the following three steps:

1. Propagating source and receiver wavefields by one-way wave equation and generate the conventional common-image gathers I and the angle-weight common-image gathers I′ using the imaging conditions of eqs. (11) and (12), simultaneously.

2. Applying the Laplacian operator to the angle-weight common-image gathers and calculating their square roots. Then the cosines of the incident-angle can be estimated by the ratios between the square roots and the amplitude values from the conventional common-image gathers I.

3) Converting the SDCIGs to ADCIGs using the incident-angle field.

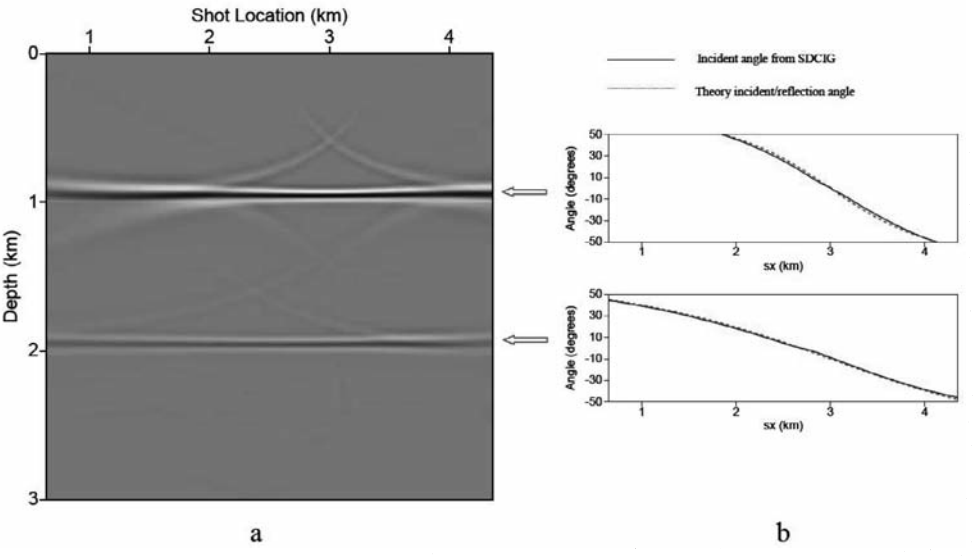

Fig. 3. SDCIG and incident-angle for location 3.0 km: (a) the SDCIG; (b) The theoretical incident-angle (dotted lines) and the calculated incident-angle from the SDCIG (solid lines) corresponds to the events from the shallow and deep part in the gather, respectively.

NUMERICAL IMPLEMENTATION

To show how this method works, we apply it to a simple model with two reflective layers (Fig. 2) with structural dips of 0° and 10°, respectively. The synthetics contain 75 shots spaced at 50 m intervals. Each shot was received with an array of 400 sensors with 10 m spacing. Fig. 3a shows a SDCIG for location 3.0 km. We estimate the incident-angle field (Fig. 3a) from the ratios between the square roots of the angle-weighted image gathers' Laplacian operators and the amplitude values from the conventional common-image gathers. The solid lines in the Fig. 3b are the incident-angles calculated by eq. (14), while the dotted lines are the exact incident-angles computed by geometry method; eq. (14) gives incident-angle information and is not dependent on structural dips.

Fig. 4 shows incident-angle field for one SDCIG. The calculated ADCIG is shown as Fig. 5b. Comparing with Fig. 5a, the ADCIG obtained by Sava and Fomel's (2003) method, the reflection events in Fig. 5b have higher resolution. Fig. 6 shows the amplitude spectrum of the angle gathers by our method (the solid line) and by the slant-stack method (the dotted line). The dominant frequency of any curve from our method is higher by 2-3 Hz than that from the

slant-stack method. This is because the Slant-stack or Radon-transform process will smooth the detail of data and lose the high-frequency components. Without this process, our method retains the bandwidth in the process of converting to angle gathers.

To verify the robustness and stability of the method, we apply it to a complicate marine structure model (Fig. 7). The subsurface geological structure includes faults, pinch outs, and alluvial fans. We first obtain the migrated section (Fig. 8) by wave equation shot-profile migration. Then we can obtain high quality ADCIGs even in a complicated structure. Fig. 9 shows a SDCIG (Fig. 9a), the incident-angle field (Fig. 9b) and the ADCIG (Fig. 9c) for location 5.5 km. The incident-angle trends are accurately displayed and a high quality angle gather is obtained in structurally complex areas with large local dip. Fig. 10 shows the ADCIGs every 125 m along the line, which demonstrates the validity and practicability of the method.

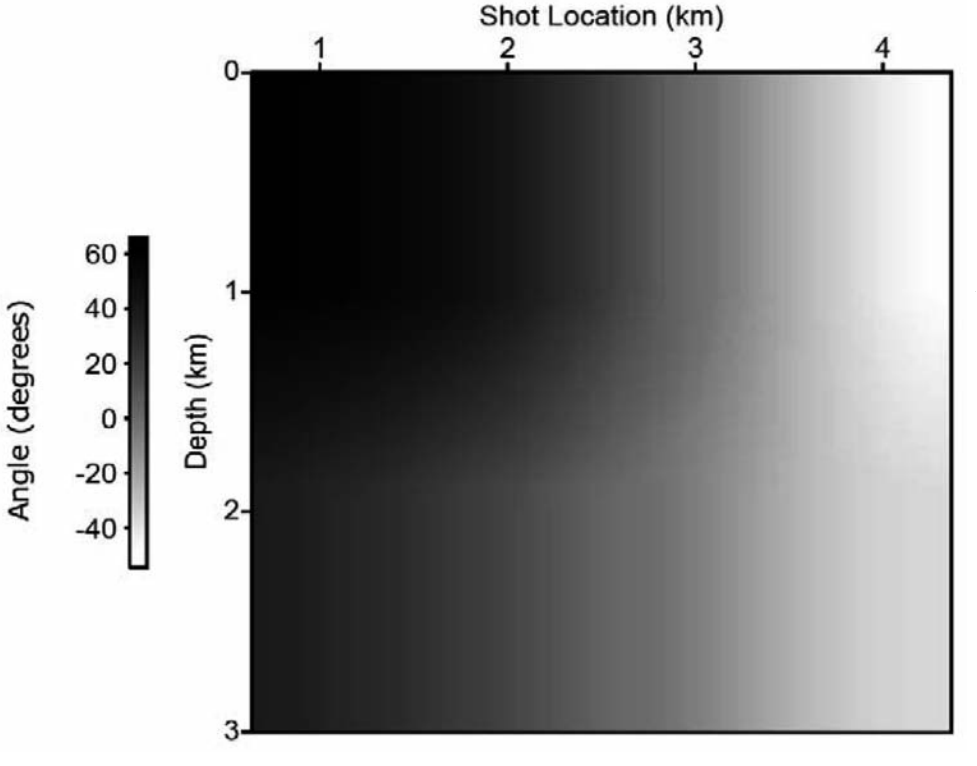

Fig. 4. The incident-angle field form SDCIG in Fig. 3.

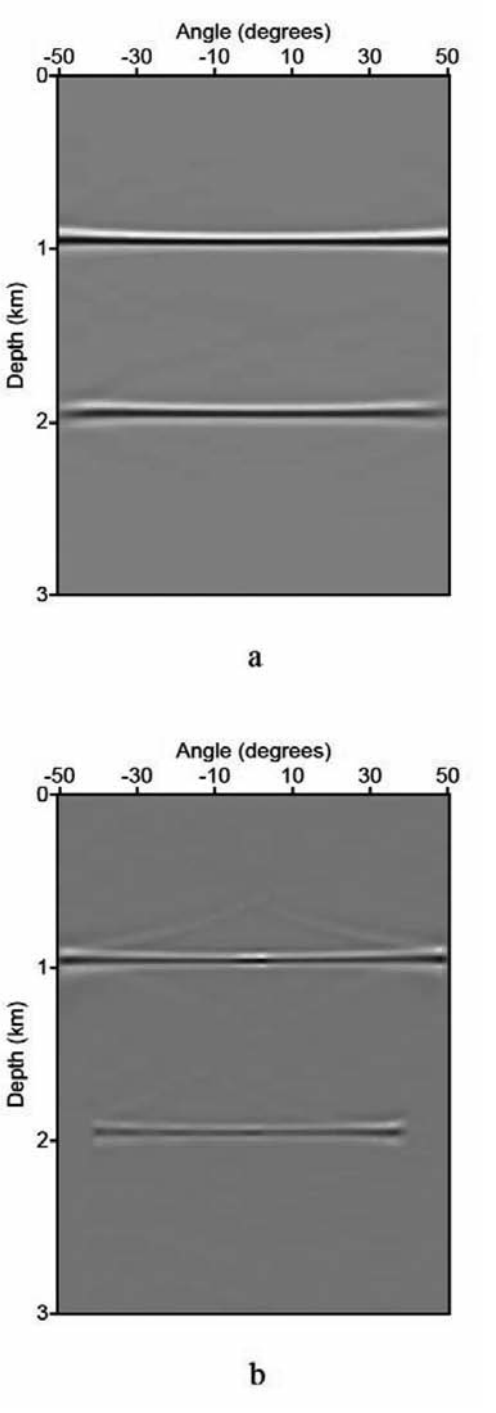

Fig. 5. The ADCIGs by (a) the slant-stack method and (b) by our method.

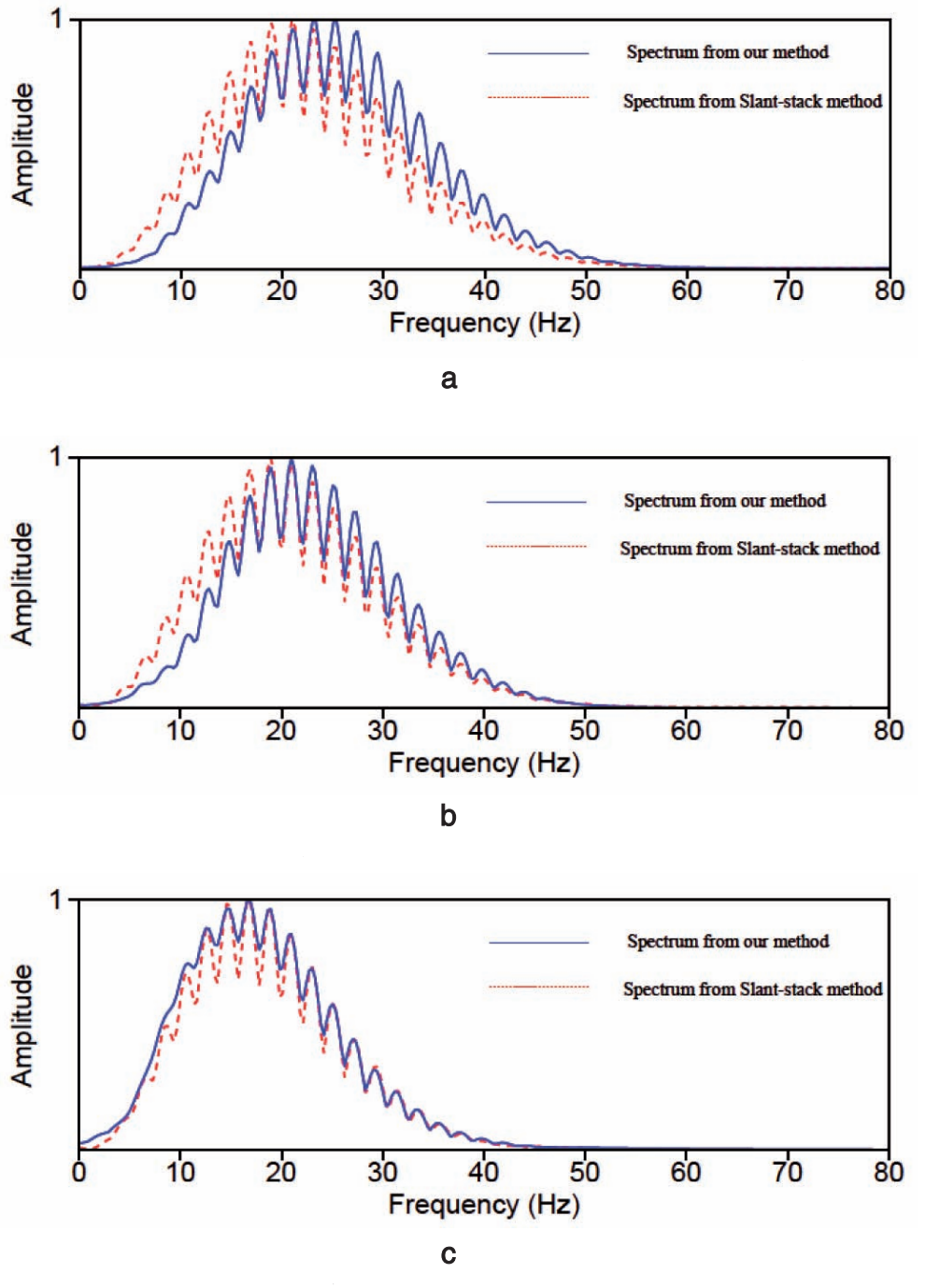

Fig. 6. The amplitude spectra of ADCIGs by our method (the solid line) and Slant-stack method (the dotted line): (a) low incident-angle part (0° - ±15°); (b) middle incident-angle part (±16° - ±35°); (c) high incident-angle part (±36° - ±50°).

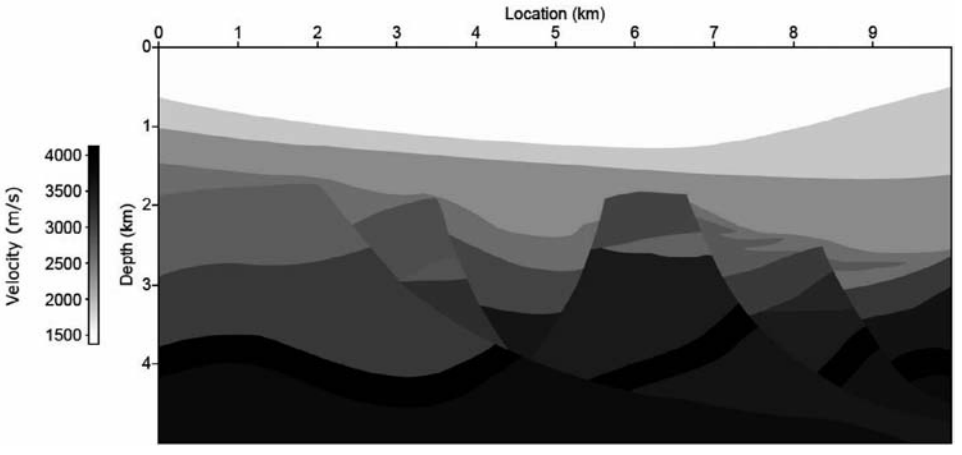

Fig. 7. Velocity of the complex structure model.

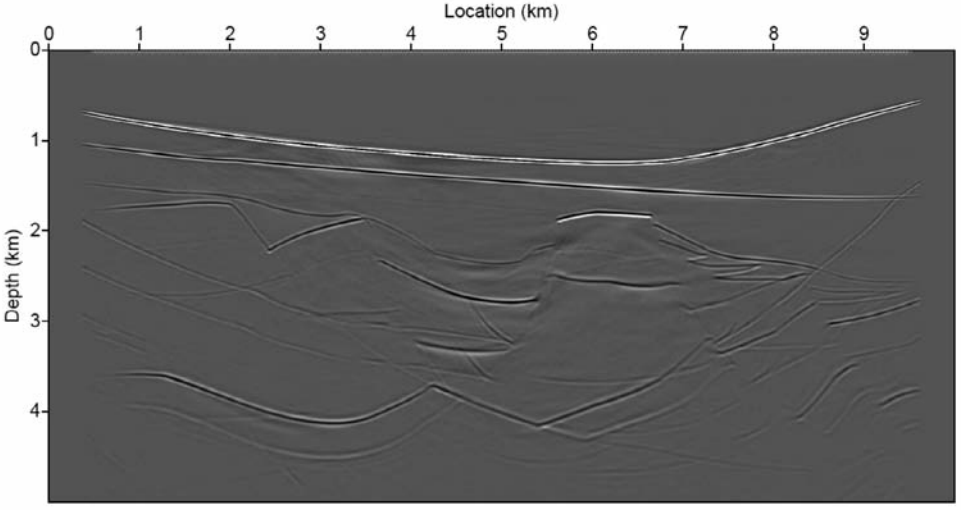

Fig. 8. The migration result of the complex structure model.

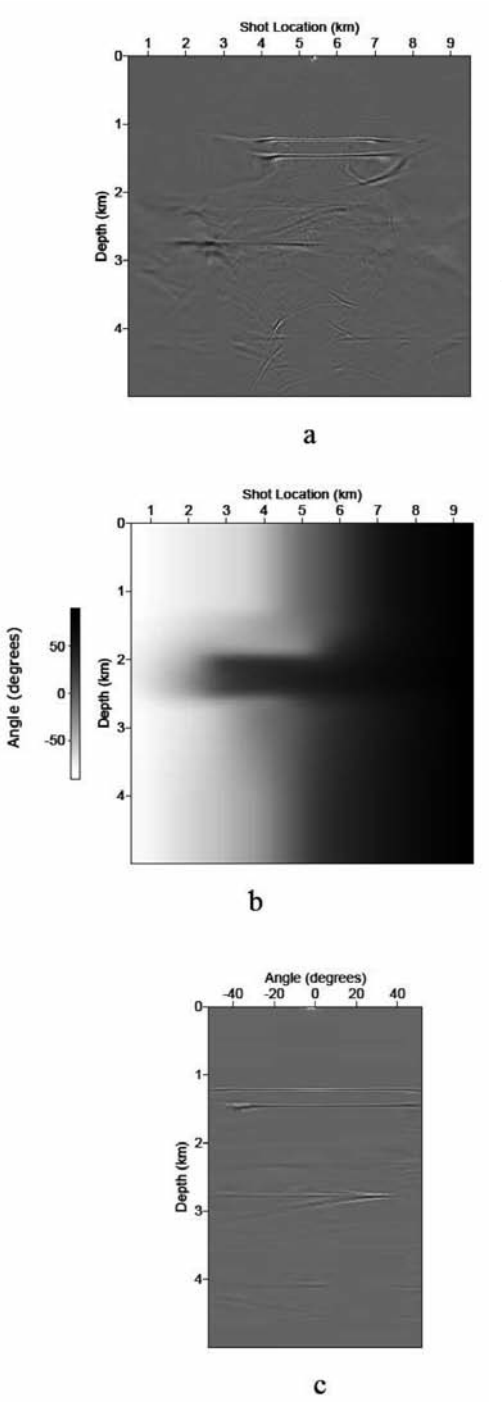

Fig. 9. Gathers located at 5.5 km: (a) SDCIG; (b) incident-angle field from SDCIG; (c) ADCIG by our method.

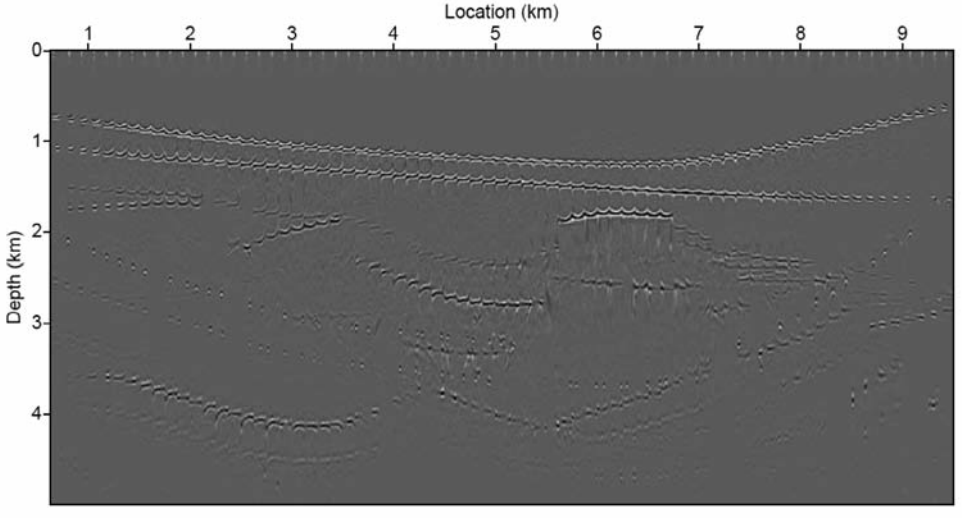

Fig. 10. The ADCIGs extracted from the model in Fig. 7 spaced at 125 m intervals.

CONCLUSIONS

We have presented a robust method to obtain ADCIGs for wave-equation shot-profile migration. It extracts ADCIGs for every imaging trace with acceptable computational cost and memory. To ensure the stability and avoid noise interference, a robust and stable division is performed at selected wave crests with large amplitude in the SDCIGs from band-limited data. The method is potentially applicable to arbitrary models, including steep dips and strong lateral velocity variations. This idea of our method can also be directly generalized to other kinds of wave-equation migration algorithms, such as reverse time migration. Numerical examples demonstrate that this method is efficient, robust and simple to implement.

ACKNOWLEDGEMENTS

This research is supported by the National Natural Science Fund of China (Grant No. 40930422), the National Major Project of China (Grant No. 2011ZX05008-006 and 2011ZX05023-005) and the China Postdoctoral Science Foundation (Grant No. 20110490575).

REFERENCES

Bleistein, N., Cohen J.K. and Stockwell, J.W., 2001. Mathematics of multidimensional seismic inversion. Springer Verlag, New York.

Biondi, B., 2006, 3D Seismic Imaging. SEG, Tulsa, OK.

Claerbout, J.F., 1985. Imaging the Earth's Interior. Blackwell Scientific Publications, Inc., New York.

De Bruin, G.G.M., Wapenaar, C.P.A, and Berkout, A.J, 1990. Angle dependent reflectivity by means of prestack migration. Geophysics, 55: 1223-1234.

Lecomte, I., 2008. Resolution and illumination analyses in PSDM: A ray-base approach. The Leading Edge, 27: 650-663.

Levin, F.K, 1971. Apparent velocity from dipping interface reflection. Geophysics, 36: 510-516.

Rickett, J. and Sava, P.C., 2002. Offset and angle-domain common imaging-point gathers for shot-profile migration. Geophysics, 67: 883-889.

Sava, P.C. and Fomel, S., 2002. Offset and angle-domain common-image gathers by wavefield continuation methods. Geophysics, 68: 1065-1074.

Sava, P.C. and Fomel. S., 2005a. Coordinate-independence angle-gathers for wave equation migration. Expanded Abstr., 75th Ann. Internat. SEG Mtg., Denver: 2052-2057.

Sava, P.C. and Fomel, S., 2005b. Wave equation common-angle gathers for converted waves. Expanded Abstr., 75th Ann. Internat. SEG Mtg., Denver: 947-950.

Shragge, J., 2012. Angle-domain common-image gathers in generalized coordinates. Geophysics, 74: S47-S56.

Slotnick, M.M., 1959. Lessons in Seismic Computing. Geyer, R.A. (Ed.). SEG, Tulsa, OK.

Xie, X.B. and Wu, R.S., 2002. Extracting angle domain information from migrated wavefield. Expanded Abstr., 72nd Ann. Internat. SEG Mtg., Salt Lake City: 1360-1363.

Yoon, K., Guo, M., Cai, J. and Wang, B., 2011. 3D RTM angle gathers from source wave propagation direction and dip of reflector. Expanded Abstr., 81st Ann. Internat. SEG Mtg., San Antonio: 3136-3140.

Zhang, Q. and McMechan, G.A., 2011. Angle domain common image gathers extracted from reverse time migrated images in isotropic acoustic and elastic media. Expanded Abstr., 81st Ann. Internat. SEG Mtg., San Antonio: 3130-3135.

Zhang, Y., Xu, S., Zhang, G. and Bleistein, N., 2005. Angle domain true amplitude wave equation migration. Extended Abstr., 67th EAGE Conf., Madrid: F045.

Zhang, Y., Xu, S., Bleistein, N. and Zhang, G., 2007. True-amplitude, angle-domain, common-image gathers from one-way wave-equation migrations. Geophysics, 72: S49-S58.